Interaction of the Sugars Trehalose, Maltose and Glucose with a Phospholipid Bilayer: A Comparative Molecular Dynamics Study

Cristina S. Pereira and Philippe H. Hünenberger*

Laboratory of Physical Chemistry, ETH-Hönggerberg, HCI, CH-8093 Zürich, Switzerland

Received: February 7, 2006; In Final Form: May 30, 2006

Molecular dynamics simulations are used to investigate the interaction of the sugars trehalose, maltose, and glucose with a phospholipid bilayer at atomic resolution. Simulations of the bilayer in the absence or in the presence of sugar (2 molal concentration for the disaccharides, 4 molal for the monosaccharide) are carried out at 325 and 475 K. At 325 K, the three sugars are found to interact directly with the lipid headgroups through hydrogen bonds, replacing water at about one-fifth to one-quarter of the hydrogen-bonding sites provided by the membrane. Because of its small size and of the reduced topological constraints imposed on the hydroxyl group locations and orientations, glucose interacts more tightly (at identical effective hydroxyl group concentration) with the lipid headgroups when compared to the disaccharides. At high temperature, the three sugars are able to prevent the thermal disruption of the bilayer. This protective effect is correlated with a significant increase in the number of sugar−headgroups hydrogen bonds. For the disaccharides, this change is predominantly due to an increase in the number of sugar molecules bridging three or more lipid molecules. For glucose, it is primarily due to an increase in the number of sugar molecules bound to one or bridging two lipid molecules.

Introduction

One of the most intriguing phenomena in biology is the occurrence of anhydrobiosis in the life cycle of some organisms such as yeasts, tardigrades, nematodes, and resurrection plants.[1] In the anhydrobiotic state, the amount of liquid water in the organism is reduced to a level where the metabolism is completely (but reversibly) stopped.[2] A common feature of anhydrobiotic processes, as well as similar processes occurring when the organism is placed under stressful temperature, pressure, osmotic, or chemical conditions, is the accumulation of large amounts of saccharides in the cell.[3,4] However, the mechanisms whereby sugars stabilize living systems during freeze−thaw, heat−cooling, or dehydration−rehydration cycles remain nowadays a matter of debate.[2,5]

In the case of anhydrobiosis, three main hypotheses have been put forward to explain the protective effect of saccharides on biomolecules. The water-replacement hypothesis suggests that during drying, sugars can substitute water molecules (in particular by forming hydrogen bonds) around the polar and charged groups present in phospholipid membranes and proteins, thereby stabilizing their native structure in the absence of water.[6−11] In particular, sugars presumably reduce the mechanical stress imposed on membranes upon dehydration and rehydration by maintaining the spacing between the headgroups and, consequently, keeping the membrane in the liquid-crystalline phase. Direct interaction between lipid and sugar molecules through the formation of hydrogen bonds has been demonstrated by several experimental techniques including infrared spectroscopy, differential scanning calorimetry, nuclear magnetic resonance (NMR), and X-ray diffraction.[6,12−20] It has also been observed in molecular simulations.[21−25] The water-entrapment hypothesis, in contrast, proposes that sugars concentrate residual water molecules close to the biomolecular surface, thereby preserving to a large extent its solvation and native properties.[26−31] This hypothesis has been formulated in the context of proteins, based on thermodynamic data in solution showing that sugars are excluded from biomolecular surfaces by water.[32,33] Finally, the vitrification hypothesis suggests that sugars found in anhydrobiotic systems (known to be good vitrifying agents) protect biostructures through the formation of amorphous glasses, thereby reducing structural fluctuations and preventing denaturation or mechanical disruption.[34−41] This hypothesis is able to provide an explanation for differences in the protecting abilities of different vitrifying agents and does not exclude the possibility of specific hydrogen bonding between lipid and sugar molecules. However, such interactions are not viewed here as a determinant factor in the stabilization process.[35,42]

In the past few years, a consensus has emerged that these mechanisms are not necessarily mutually exclusive.[2−4,38,43] Vitrification may occur simultaneously with a direct interaction of the sugar with the biostructure or with an entrapment of residual water at its surface, depending on the type of the protected biostructure and on the nature of the environmental stress.

In the context of membrane dehydration and rehydration (based on experiments using liposomes), it appears that two requirements must be fulfilled to achieve an efficient stabilization: (i) a significant depression of the gel to liquid-crystalline phase transition temperature T_m of the dried phospholipids induced by the sugar[8,43−45] and (ii) a high glass transition temperature T_g of the protecting sugar.[34,35,38] The first requirement implies the inhibition of the transition to the gel phase upon dehydration. This transition generally occurs in the absence of sugar, because the T_m of a dry phospholipid bilayer is typically much higher than the corresponding value at full hydration. For instance, dipalmitoylphosphatidylcholine (DPPC) has a T_m of 42 °C in the hydrated state, which rises to nearly 120 °C when the lipid is fully dehydrated.[46] However, the T_m

* Corresponding author. Phone: +41-1-632-5503. Fax: +41-1-632-1039. E-mail: phil@igc.phys.chem.ethz.ch.

10.1021/jp060789l CCC: $33.50
Published on Web 07/18/2006

of the same dried phospholipid is only 55 °C in the presence of trehalose.[45] This first requirement appears to be directly correlated with the presence of sugar−headgroup hydrogen bonds.[43,45,47] The second requirement corresponds to good vitrification properties of the sugar, implying the formation of a glassy matrix over the range of concentrations where the system becomes unstable during dehydration.[34,35,38] For instance, trehalose and maltose (with T_g values of 116.9 and 100.6 °C[48] in the absence of water) have significantly better vitrification properties than glucose with a T_g of 38.2 °C.[48] In liposome experiments, this second requirement appears sufficient to prevent membrane fusion upon dehydration, while the two conditions must be fulfilled simultaneously to prevent leakage of the liposome content upon rehydration.[45,47]

In the present work, a theoretical method is used to compare the effect of trehalose (TRH), maltose (MLT), and glucose (GLC) on the structure and dynamics of a DPPC bilayer in the liquid-crystalline phase. Molecular dynamics (MD) simulations of the bilayer in the absence or in the presence of TRH, MLT, and GLC are performed at two different temperatures (325 and 475 K), so as to provide a better understanding of sugar−membrane interactions, their variations along this series of saccharides, and their response when the membrane is exposed to unfavorable conditions (mimicked here by an artificially elevated temperature).

Among the three sugars considered, only TRH is used by nature to promote bioprotection in organisms able to survive severe external stresses.[49] Studies on the metabolism of yeasts,[50−52] tardigrades,[53,54] nematodes,[55,56] resurrection plants,[57,58] and *Artemia* species[59−61] have shown that these organisms accumulate TRH in large concentrations during anhydrobiosis, heat shock, or osmotic stress. Even though MLT and GLC are not used by nature during anhydrobiosis, they have been tested in vitro (often in comparison to TRH) for the protection of biomolecules and biostructures exposed to stress factors.[14,15,45,47,62−67] Most of these comparative studies show that MLT may be as effective as TRH in preserving biological activity in lyophilized membranes and liposomes.[62,63,66,67] In contrast, GLC is found to be significantly less effective than MLT and TRH.[14,15,45,47,62,63,65−67] It has been suggested that, although GLC shows direct hydrogen-bonding interaction with the phospholipid headgroups and efficiently depresses the gel to liquid-crystalline phase transition temperature,[47] it is not a sufficiently good vitrifying agent and does not efficiently prevent membrane fusion due to its significantly lower glass transition temperature.[14,43−45,47]

Structural and hydration properties of the three sugars have been extensively investigated in previous studies. TRH and MLT are isomeric disaccharides of GLC; MLT involves an α(1→4) glycosidic bond, while TRH presents an α(1→1) linkage, leading to a nonreducing sugar. Several experimental[68−72] and theoretical[73−77] studies have investigated the solution properties of TRH, MLT, and GLC aiming at a better understanding of the connection between the structural and solvation properties of these sugars and their bioprotective abilities. Sugars are believed to have a destructuring effect on the hydrogen-bond network of water.[69−71] In particular, TRH seems characterized by a more extended hydration as compared to other disaccharides and binds water molecules more strongly.[69−75] In addition, this disaccharide seems to have a similar ability to interact with both sugar and water molecules, making TRH−water systems more homogeneous.[74] These particularities of TRH−water interactions could be related to the high biopreservative efficiency of this sugar.[69,74]

Methods

The computational methods used in the present work have been described in detail in a previous study restricted to TRH−membrane interaction[22] and will only be summarized here.

Molecular Dynamics Simulations. All MD simulations were performed using the GROMOS96 program[78] together with the GROMOS96 45A4 force field including new parameters developed for lipids[79] and carbohydrates,[80] and the SPC water model.[81] All parameters used in the present MD simulations involving TRH, MLT, or GLC as cosolutes were identical to those used in our previous study involving only TRH,[22] with a single exception: the previous simulations relied on an earlier (preliminary) version of the carbohydrate force field (differing by specific dihedral-angle potentials in the TRH molecule).[22] For this reason, simulations involving TRH were repeated here using the latest (published) 45A4 force-field version.[80] The new results are in excellent qualitative (although not quantitative) agreement with the earlier ones, and no modification is required to the main conclusions drawn in our previous article.[22] Only the results of the simulations involving TRH at 2 molal (m) concentration are discussed in the present article. For completeness, the corresponding results for the new simulations involving TRH 1 m are provided as Supporting Information.

Molecular Systems. A hydrated membrane bilayer of 2 × 64 DPPC molecules was simulated in the absence or in the presence of the different sugars, and at two different temperatures (325 and 475 K). A total of eight simulations were performed involving: (i) the DPPC bilayer in pure water at 325 or 475 K (control simulations); (ii) the DPPC bilayer in a 2 m TRH solution (128 TRH molecules) at 325 or 475 K; (iii) the DPPC bilayer in a 2 m MLT solution (128 molecules) at 325 or 475 K; and (iv) the DPPC bilayer in a 4 m GLC solution (256 molecules) at 325 or 475 K.

The highest temperature is not meant to represent a physical situation. It is merely used here to investigate how sugars affect the response of the bilayer to stress conditions. The concentration of the GLC solution is twice higher than that of the TRH and MLT solutions, so as to keep roughly the same effective concentration of hydroxyl groups while exclusively varying the connectivity of the carbon backbone. This allows for a direct investigation of the effect of configurational restrictions imposed by a given molecular framework on the capacity of the compound to interact with the membrane.

A DPPC bilayer at full hydration (3655 water molecules, i.e., 28−29 water molecules per lipid) in the liquid-crystalline phase, previously equilibrated during a 2.5 ns MD simulation at 325 K, was used as the initial structure for all simulations. This configuration was taken without alterations for the production runs corresponding to the simulations in the absence of sugar. For the simulations including sugars, the water molecules were removed and 128 (2 m solution, for TRH and MLT) or 256 sugar molecules (4 m solution, for GLC) were uniformly distributed in the system, maintaining a distance of at least 0.5 nm from each other and from the two surfaces of the bilayer. The systems were then resolvated using 3339 water molecules (resulting in 26−27 water molecules per lipid), imposing a minimum distance of 0.28 nm between water molecules and any solute atom. The initial box dimensions were approximately the same for all systems containing sugars: TRH (5.8 × 6.2 × 8.5 nm), MLT (5.9 × 6.1 × 8.4 nm), and GLC (5.8 × 6.3 × 8.5 nm), where the last dimension (*z*-axis) refers to the bilayer normal. In the absence of sugar, the box dimensions were 5.8 × 6.2 × 7.3 nm.

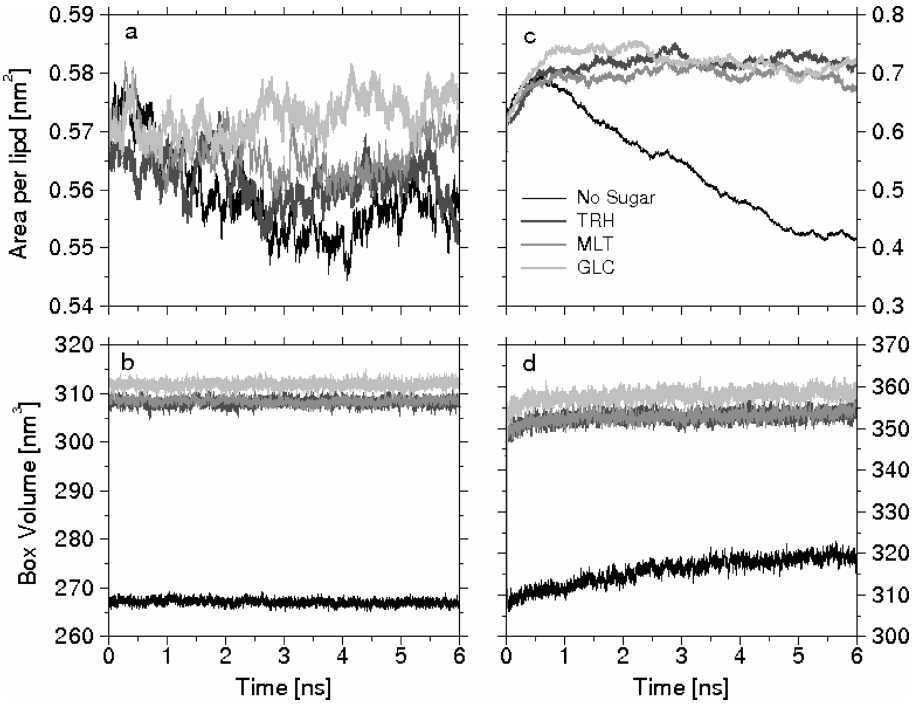

Figure 1. Area per lipid (a,c) and box volume (b,d) as a function of time, for the four simulations of a DPPC bilayer in the absence or in the presence of different sugars (2 m TRH, 2 m MLT, or 4 m GLC) at 325 K (a,b) and at 475 K (c,d).

All simulations involving GLC relied on a model representative of the β-anomer only. Although it is known that GLC solutions present two anomers at equilibrium (ca. 62% β-D-glucose and 38% α-D-glucose[82]), the restriction to a single anomeric form is not likely to significantly affect the main conclusions drawn from the present simulations, due to the close structural similarity of the two anomers. The simulations involving MLT considered the α-anomer.

Equilibration. For the systems without sugar, the configuration equilibrated at 325 K during 2.5 ns was used directly to initiate two 6 ns production simulations, either at the same temperature or at an increased temperature of 475 K. For the systems including sugars, a thorough equilibration procedure (involving in particular the relaxation of the sugar−water mixture by a 5 ns simulation at 500 K with positional restraints on the lipid molecules) was first performed as described in detail in our previous study.[22] This equilibration was followed by 6 ns production simulations at 325 or 475 K.

Analyses. The analyses performed in this work were the same as those described in our previous study[22] and involved the average area per lipid for the DPPC molecules, the deuterium order parameters (S_{CD}) for the two acyl chains of DPPC (sn-1 and sn-2), the normalized density profiles for specific atoms of DPPC (phosphorus, nitrogen, and the glycerol CH_1 united atom), TRH (glycosidic oxygen), MLT (glycosidic oxygen), GLC (lactol oxygen), and water (oxygen atom) along the bilayer normal (*z*-axis of the simulation box), the lateral (*xy*-plane of the simulation box) diffusion coefficients (D_{xy}) for DPPC, TRH, MLT, GLC, and water molecules (same reference atom for water and sugars, glycerol CH_1 united atom for DPPC), the hydrogen bonds (H-bonds), classified according to the pairs of species present in the simulated systems, and the patterns of sugar−DPPC H-bonding presented by the different sugar molecules.

Results and Discussion

Simulations at 325 K. At 325 K, the area per lipid for the DPPC bilayer in the presence of sugars is slightly increased as compared to the simulation in their absence (Figure 1a). However, the corresponding values of 0.56, 0.56, 0.57, and 0.58 nm^2 (averaged over the last 1 ns of the simulations without sugar and with TRH, MLT, and GLC, respectively) are in the expected range for a fully hydrated DPPC membrane in the liquid-crystalline phase.[83] The slight expansion of the membrane in the presence of sugars, if it can be considered meaningful (given the fluctuation in this quantity and the short time scale of the simulations[22]), agrees qualitatively with experimental studies of DPPC bilayers (as well as bilayers involving other lipids), suggesting that sugar molecules intercalate between the lipid headgroups, thereby increasing the spacing between the lipid chains.[13,16,84] A similar trend, but of significantly larger magnitude, was also reported in a study involving DPPC monolayers.[17] However, the similitude between monolayers and bilayers in this context remains a matter of debate.[16,25] The time evolution of the box volume is essentially constant in the four simulations (Figure 1b), indicating that equilibrium has been reached for the average system density.

At 325 K, the ordering of the lipid chains is only weakly affected by the presence of sugars, as can be seen from the order parameters (S_{CD}) calculated for the consecutive atoms of the sn-1 and sn-2 chains of DPPC (Figure 2a,b). The order parameters for the sn-1 chain slightly decrease upon inclusion of TRH or GLC, while they remain unaltered in the presence of MLT. For the sn-2 chain, the three sugars slightly decrease the order parameter of carbon atoms close to the headgroups. However, TRH promotes order in the tail region, GLC promotes disorder, while MLT has no effect. Note that the S_{CD} values for the sn-2 chain in the absence of sugar are somewhat overestimated as compared to experimental data,[85] a known feature of the lipid force field employed in the present simulations.[79]

The mobility of water, TRH, MLT, GLC, and DPPC molecules in the different systems can be analyzed on the basis of the calculated lateral diffusion coefficients (D_{xy}) for these species (Table 1). The value of D_{xy} for water in the absence of sugar (4.80×10^{-5} cm^2 s^{-1}) is somewhat higher than the experimental value $D = 3.47 \times 10^{-5}$ cm^2 s^{-1}at 323 K,[86] a

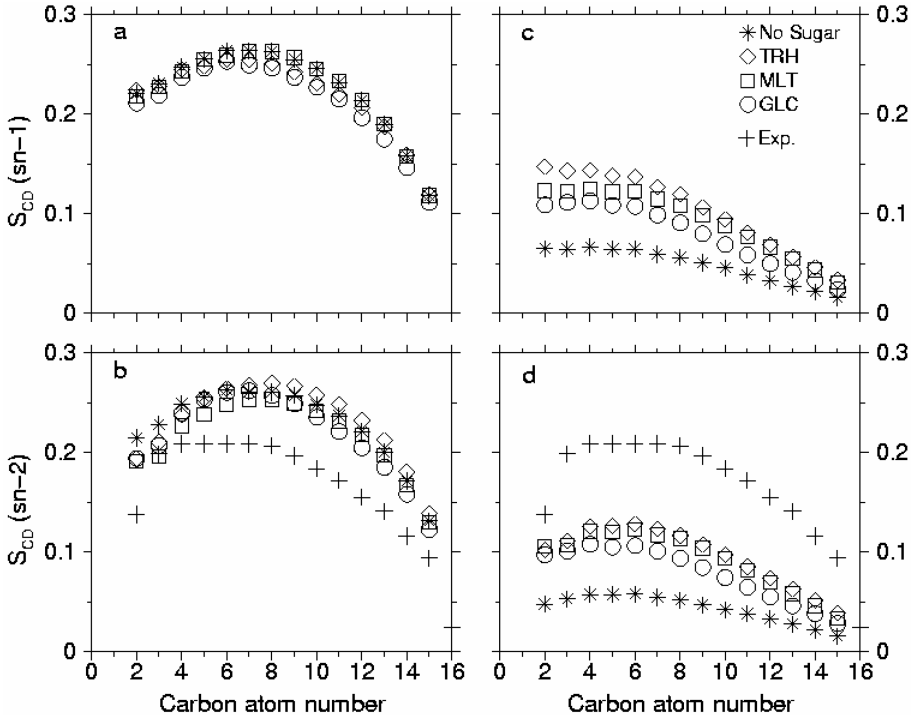

Figure 2. Deuterium order parameters (S_{CD}) as a function of the carbon atom number along the sn-1 and sn-2 chains of DPPC, calculated for the four simulations of a DPPC bilayer in the absence or in the presence of different sugars (2 m TRH, 2 m MLT, or 4 m GLC) at 325 K for the sn-1 (a) and sn-2 (b) chains, and at 475 K for the sn-1 (c) and sn-2 (d) chains. Experimental values for the sn-2 chain at 325 K[72] are reported for comparison. The values are averaged over 128 DPPC molecules and over the 6 ns simulation time.

TABLE 1: Lateral Diffusion Coefficients (D_{xy}) for Water, TRH, MLT, GLC, and DPPC Molecules during the Four Simulations of a DPPC Bilayer in the Absence or in the Presence of Different Sugars (2 m TRH, 2 m MLT, or 4 m GLC) at 325 and 475 K[a]

		325 K	475 K
sugar		D_{xy} [10^{-5} cm^2 s^{-1}]	D_{xy} [10^{-5} cm^2 s^{-1}]
none	water	4.80	17.14
	DPPC	0.014	0.273
TRH	water	2.61	15.87
	DPPC	0.026	0.470
	TRH	0.10	1.19
MLT	water	2.32	15.19
	DPPC	0.010	0.170
	MLT	0.12	0.96
GLC	water	2.46	14.75
	DPPC	0.030	0.393
	GLC	0.29	2.19

[a] The values reported for TRH 2 m are comparable to those observed in our previous study using an earlier version of the carbohydrate force field[22] (due to a typographical mistake; the data for D_{xy} and D_z at 475 K in Table 1[22] therein should be divided by a factor of 10). The corresponding data for TRH 1 m based on the final (published) force field version are provided as Supporting Information.

known feature of the SPC water model.[79] This diffusion coefficient decreases by about a factor of 2 upon adding any of the three sugars to the solution. The diffusion coefficient of GLC is higher than the ones of MLT and TRH by a factor of 2.5−3.0, which can be explained by the smaller size of the GLC molecule. The values of D_{xy} for water (2.61×10^{-5} cm^2 s^{-1}) and TRH (0.10×10^{-5} cm^2 s^{-1}) in the 2 m TRH solution are in qualitative agreement with experimental results for the diffusion of water ($D = 1.05 \times 10^{-5}$ cm^2 s^{-1}) and TRH ($D = 0.151 \times 10^{-5}$ cm^2 s^{-1}) in a 44% TRH solution (2.10 m) at 323 K.[86] The calculated values for the lateral diffusion of DPPC are of the same order of magnitude as those obtained from neutron scattering measurements ($D_{lat} = 0.01 \times 10^{-5}$ cm^2 s^{-1}).[87] In contrast to the water molecules, this coefficient increases approximately by a factor of 2.5−3.0 upon adding TRH or GLC to the system (although it remains essentially unchanged upon adding MLT). However, it should be stressed that these coefficients are only indicative, because the mean-square positional displacement of DPPC molecules is only approximately linear in time on the 6 ns time scale. The limited changes observed in the mobility of the three species indicate that the systems are still in a diffusive (as opposed to glassy) state in the presence of the sugars at the selected concentrations.

The distributions of specific DPPC, TRH, MLT, GLC, and water atoms along the bilayer normal, averaged over the last 0.25 ns of the simulations (Figure 3a−d), show that the membrane remains intact in all cases, although the distributions of the lipid atoms are somehow broader in the presence of the sugars. Many sugar molecules interact tightly with the membrane as evidenced by the density peaks observed for TRH, MLT, and GLC in the vicinity of the bilayer surfaces and the overlap between these peaks and those corresponding to DPPC headgroup atoms. However, water molecules are not completely excluded from the membrane surface upon coating by sugar molecules.

The total number of H-bonds present on average between the different species in the system, together with this quantity scaled by the total number of interacting partners, are reported in Table 2 for TRH, Table 3 for MLT, and Table 4 for GLC. The latter quantity indicates the expected number of H-bonds between any two molecules of the corresponding species selected at random in the system (reported in percent). Among all species present in the simulations involving disaccharides (TRH or MLT), the highest H-bonding probability is found for pairs involving two sugar molecules. This result certainly indicates a high H-bonding affinity among sugar molecules, but is also related to the fact that disaccharides contain a large number of groups capable of forming H-bonds. In contrast, for

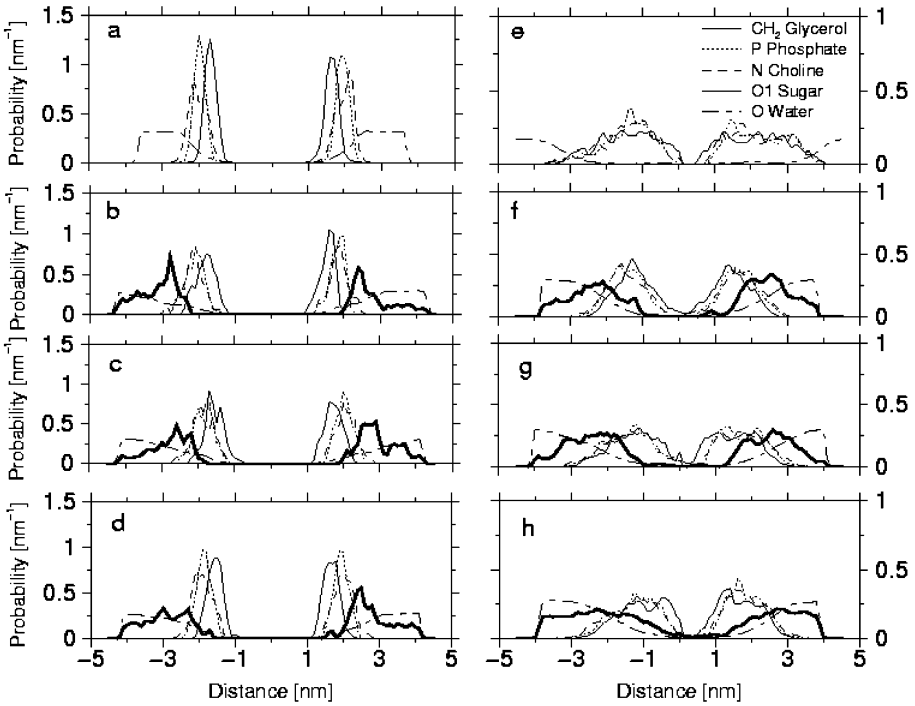

Figure 3. Normalized density profiles for specific DPPC, sugar, and water atoms along the bilayer normal (*z*-axis) calculated for the four simulations of a DPPC bilayer in the absence of sugar (a,e), or in the presence of 2 m TRH (b,f), 2 m MLT (c,g), or 4 m GLC (d,h), at either 325 K (left panels) or 475 K (right panels). The profiles correspond to averages over the last 0.25 ns of each simulation.

TABLE 2: Average Number of H-Bonds and Probability of H-Bond Formation between All Species Present in the Simulations of a DPPC Bilayer in the Absence of Sugar or in the Presence of 2 m TRH at 325 and 475 K[a]

	TRH−DPPC	TRH−TRH	TRH−water	DPPC−water	
C_{TRH}	2 m	2 m	2 m	0 m	2 m
		325 K			
H-bonds	96.07	161.71	1356.10	552.06	413.91
S.D.	6.32	10.93	27.14	12.38	10.18
probability [%]	0.586	0.987	0.317	0.118	0.097
S.D. [%]	0.039	0.067	0.006	0.003	0.002
		475 K			
H-bonds	158.46	106.56	892.13	295.21	275.98
S.D.	12.28	10.43	30.80	36.79	17.87
probability [%]	0.936	0.655	0.209	0.063	0.065
S.D. [%]	0.115	0.065	0.007	0.008	0.004

[a] Standard deviations (S.D.) are reported for the two quantities. The averages are calculated over the interval 2.0−6.0 ns for each simulation. The values reported for 2 m TRH are comparable to those observed in our previous study using an earlier version of the carbohydrate force field,[22] except for a significantly lower number of TRH−TRH H-bonds. The corresponding data for 1 m TRH based on the final (published) force field version are provided as Supporting Information.

TABLE 3: Average Number of H-Bonds and Probability of H-Bond Formation between All Species Present in the Simulations of a DPPC Bilayer in the Absence of Sugar or in the Presence of 2 m MLT at 325 and 475 K[a]

	MLT−DPPC	MLT−MLT	MLT−water	DPPC−water	
C_{MLT}	2 m	2 m	2 m	0 m	2 m
		325 K			
H-bonds	117.04	169.54	1334.10	552.06	399.73
S.D.	9.68	10.77	26.29	12.38	13.34
probability [%]	0.714	1.035	0.312	0.118	0.094
S.D. [%]	0.059	0.657	0.006	0.003	0.003
		475 K			
H-bonds	169.64	132.86	858.61	295.21	256.83
S.D.	13.01	11.30	31.40	36.79	18.05
probability [%]	1.035	0.811	0.201	0.063	0.060
S.D. [%]	0.079	0.069	0.007	0.008	0.004

[a] Standard deviations (S.D.) are reported for the two quantities. The averages are calculated over the interval 2.0−6.0 ns for each simulation.

the simulations involving GLC, the highest probability is found for GLC−DPPC pairs. This is not only due to a reduction in the number of potential H-bonding groups in GLC−GLC pairs (by about a factor of four as compared to disaccharides, while this number is only halved for GLC−DPPC pairs), but also related to an increase in the absolute number of sugar−DPPC H-bonds as compared to the disaccharide case (see below).

In the three systems involving sugars, the sum of the sugar−DPPC and water−DPPC H-bonds (509.98, 516.77, and 530.82 for TRH, MLT, and GLC, respectively) is almost equal to the number of water−DPPC H-bonds in the system without sugar (552.06). Water is not completely excluded from the membrane surface upon coating by the sugars and still forms many H-bonds with the lipid headgroups, but sugar molecules appear to replace water at about one-fifth to one-quarter of the H-bonding sites provided by the membrane surface.

The average number of sugar−DPPC H-bonds (at almost identical effective hydroxyl-group concentration) increases in the order TRH < MLT ≪ GLC. The higher H-bonding capacity of GLC is expected due to the smaller size of the molecule (better intercalation between headgroups) and the reduced topological constraints imposed by the molecular framework on the relative locations and orientations of the hydroxyl groups. The closer approach between GLC and the lipid headgroups (as compared to TRH and sucrose) was also observed experimentally in an infrared-spectroscopy study,[88] suggesting that the membrane in the presence of GLC may be more fragile under mechanical stress.[88]

Sugar−headgroup H-bonds involve sugar hydroxyl groups and oxygen acceptors of either the phosphate or the ester groups of the lipid molecules. As shown in Table 5, the leading contribution (about 80%) is provided by sugar−phosphate H-bonds, in agreement with experimental data on the interaction

TABLE 4: Average Number of H-Bonds and Probability of H-Bond Formation between All Species Present in the Simulations of a DPPC Bilayer in the Absence of Sugar or in the Presence of 4 m GLC at 325 and 475 K[a]

	GLC−DPPC	GLC−GLC	GLC−water	DPPC−water	
C_{GLC}	4 m	4 m	4 m	0 m	4 m
		325 K			
H-bonds	155.41	199.95	1709.80	552.06	375.41
S.D.	9.22	14.12	31.19	12.38	11.07
probability [%]	0.474	0.305	0.200	0.118	0.400
S.D. [%]	0.028	0.022	0.003	0.003	0.007
		475 K			
H-bonds	217.17	125.79	1119.80	295.21	251.45
S.D.	13.73	12.98	34.35	36.79	20.83
probability [%]	0.663	0.192	0.131	0.063	0.059
S.D. [%]	0.042	0.020	0.004	0.008	0.005

[a] Standard deviations (S.D.) are reported for the two quantities. The averages are calculated over the interval 2.0−6.0 ns for each simulation.

TABLE 5: Average Number and Relative Contribution to the Total Number of Sugar-Headgroups H-Bonds Formed between Sugar Hydroxyl Groups and Oxygen Atoms from Either the Phosphate or the Ester Group of the Lipid Molecules[a]

	H-bonds to phosphate	H-bonds to ester	H-bonds to phosphate [%]	H-bonds to ester [%]
		325 K		
TRH−DPPC (2 m)	84.08	11.99	87.53	12.47
MLT−DPPC (2 m)	96.48	20.56	82.43	17.57
GLC−DPPC (4 m)	114.67	40.74	73.79	26.21
		475 K		
TRH−DPPC (2 m)	93.43	65.03	58.96	41.04
MLT−DPPC (2 m)	106.43	63.21	62.74	37.26
GLC−DPPC (4 m)	112.62	104.55	51.85	48.15

[a] The averages are calculated over the interval 2.0−6.0 ns for each simulation.

of sugars with lipids.[6,13,16,17,19,20,45,47,84] Interestingly, the relative contribution of sugar−ester H-bonds is higher for GLC as compared to MLT or TRH, probably again due to the smaller size and better intercalation properties of the monosaccharide. The presence of TRH−ester H-bonds was also observed in a previous simulation study where this feature was suggested to correlate with a predominant orientation of TRH molecules at the bilayer surface with their main axis parallel to the lipid chains.[23]

The present findings at 325 K are in excellent qualitative agreement with the results of independent recent MD simulations investigating the interaction of TRH with phospholipid bilayers at similar temperature.[21,23−25]

Simulations at 475 K. At 475 K, the area per lipid of the DPPC bilayer initially expands (by about 20% within 1 ns). The subsequent evolution of this quantity depends on the presence or absence of sugar (Figure 1c). A large decrease in the bilayer area (44%) is observed during the simulation without sugar. In contrast, the simulations with sugars are characterized by an almost constant area per lipid over the final 5 ns of the simulations. The corresponding values of 0.72, 0.70, and 0.72 nm^2 (averaged over the last 5 ns of the simulations with TRH, MLT, and GLC, respectively) are, however, significantly higher than the best experimental estimate of 0.64 nm^2 for a fully hydrated DPPC membrane in the liquid-crystalline phase at 325 K.[83] The time evolution of the box volume (Figure 1d) shows that the temperature increase leads to an overall expansion of the systems (with or without sugar).

The distributions of specific DPPC and water atoms along the bilayer normal, averaged over the last 0.25 ns of the simulation without sugar (Figure 3e), provide the explanation for the important decrease in the area per lipid. In this simulation, the bilayer structure is nearly entirely disrupted (compare with Figure 3a at 325 K). The distributions of the headgroup and glycerol atoms are largely broadened and almost completely overlap. The clear separation between the two layers is no longer observed, and the water distribution extends over the entire range of distances. In contrast, upon inclusion of TRH, MLT, or GLC, the bilayer structure is preserved during the entire simulation (Figure 3f−h). Despite the somewhat broadened probability distributions for the lipid atoms (as compared to 325 K; Figure 3b−d), the membrane can be clearly recognized as a bilayer. The integrity of the bilayer appears to be slightly better preserved in the presence of TRH molecules (Figure 3f) as compared to MLT (Figure 3g) or GLC (Figure 3h). As was the case at 325 K, the distributions evidence a high affinity of sugar molecules for the bilayer surfaces, but only limited desolvation of the lipid headgroups upon sugar coating. In a simulation study of cholesterol-containing DPPC bilayers in the presence of TRH at different temperatures, it was also found that even at high cholesterol concentrations, TRH is able to interact with the phospholipid headgroups and to inhibit some changes in the lateral organization of the bilayer components that would be induced by the presence of cholesterol molecules.[89]

The different behavior of the bilayer during the high-temperature simulations is clearly visible in the final configurations of the four 6 ns simulations (Figure 4). The thermally induced disruption of the membrane in the absence of sugar is evident in Figure 4a. The three sugars are able to reduce the disruptive effect of the temperature. The bilayer integrity appears to be slightly better preserved in the presence of TRH (Figure 4b) than in the presence of MLT (Figure 4c) or GLC (Figure 4d).

The analysis of the order parameters (S_{CD}) at 475 K shows how the ordering of the DPPC sn-1 and sn-2 chains is affected by the different sugars (Figure 2c,d). In the absence of sugar, the disorder of the chains is considerably enhanced as compared to the results at 325 K and to the experimental data for the sn-2 chain, a consequence of the increased thermal motion and of the membrane disruption. The order parameters significantly increase upon adding a sugar to the system. TRH is most efficient at reducing the chain disorder, while GLC is the least efficient of the three sugars. For both chains, the sugar-induced order increase is more evident for the carbon atoms close to the headgroups. Although the simulations in the presence of sugar are characterized by a stable bilayer structure, the corresponding order parameters remain significantly lower as compared to the corresponding simulation at 325 K and to experiment. This is certainly a consequence of both the elevated temperature and the concomitant increase in the area per lipid.

The lateral diffusion coefficients for water, TRH, MLT, GLC, and DPPC molecules (Table 1) are 1−2 orders of magnitude higher than the corresponding values at 325 K, a consequence of the increased thermal motion. At this elevated temperature, the diffusion of water molecules is only weakly affected by the presence of sugar in the system. Comparing the values at 475 K for the systems with and without sugars, there is a decrease in the lateral diffusion coefficient of DPPC upon including MLT, but an increase upon including TRH or GLC (however, this quantity may not be entirely converged in the present simulations). The diffusion coefficient of GLC is about twice the one of TRH and MLT, as was the case at 325 K. Because the inclusion of the sugars does not induce order-of-magnitude changes in the diffusional dynamics of the systems at 475 K, it is unlikely that the preservation of the membrane structure in

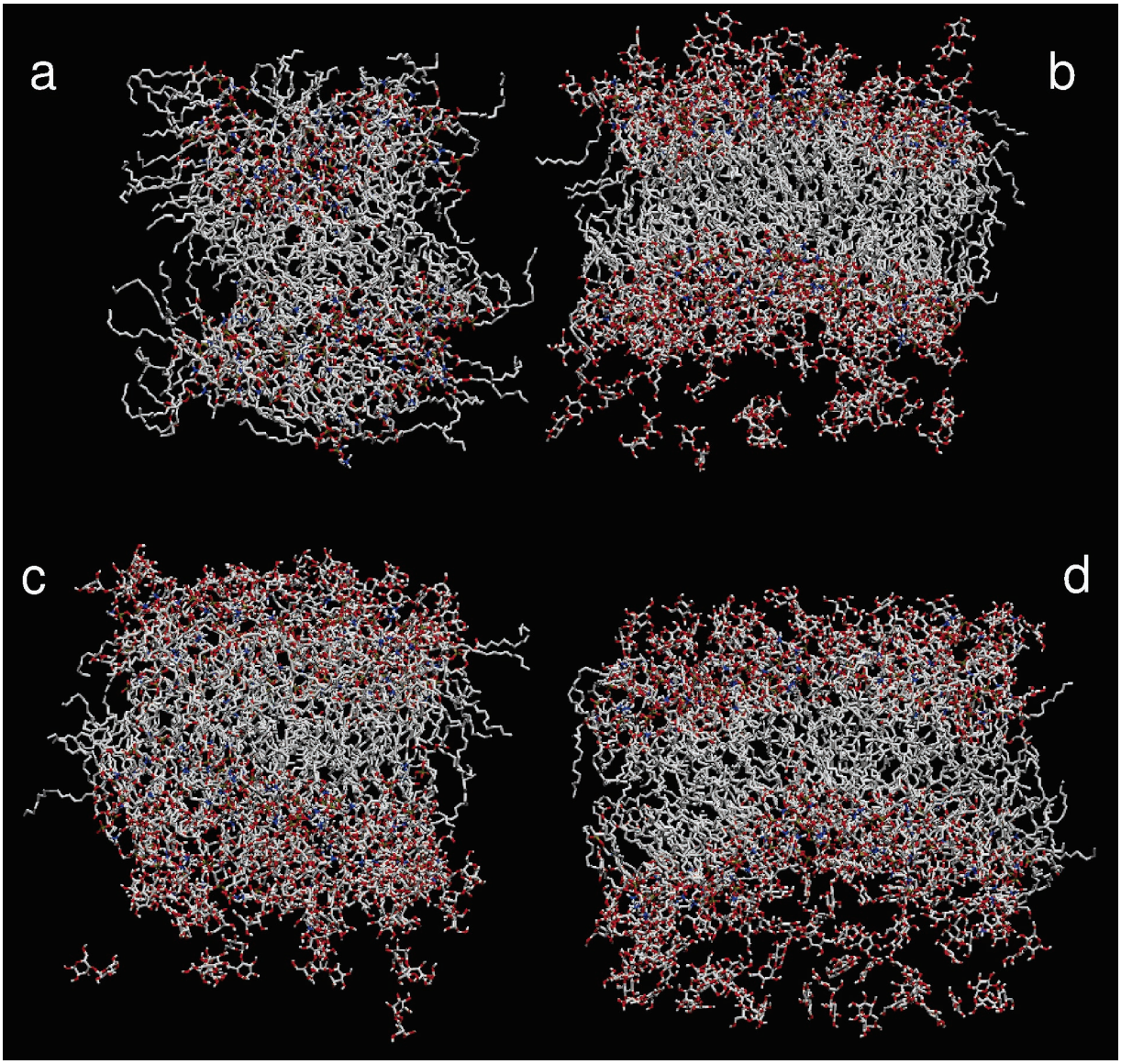

Figure 4. Final configurations of the systems at 475 K (a) without sugar, (b) with 2 m TRH, (c) with 2 m MLT, and (d) with 4 m GLC. All molecules are represented using a stick model. Water molecules have been removed for clarity. Carbon atoms are represented in gray, oxygen atoms in red, phosphorus atoms in yellow, nitrogen atoms in blue, and hydrogen atoms in white.

the presence of sugars is merely a kinetic effect (membrane disruption taking longer than the 6 ns simulation time). Rather, the membrane preservation appears to result from a thermodynamically increased stability.

The H-bond analysis for the simulations at 475 K (Tables 2−4) reveals an overall decrease (47% for the system without sugar and about 30% for the three systems containing a sugar) in the total number of H-bonds as compared to the simulations at 325 K, as expected from the increased thermal motion. The decrease is also evident in the sugar−sugar, sugar−water, and DPPC−water components taken individually. For example, the number of DPPC−water H-bonds decreases upon increasing the temperature by 33%, 35%, and 33% for the systems with TRH, MLT, and GLC, respectively. Interestingly, however, the number of sugar−DPPC H-bonds shows exactly the opposite trend, increasing by 65%, 45%, or 40%, for the systems with TRH, MLT, or GLC, respectively. This increase appears to be thermodynamically driven, rather than being a mere consequence of a faster diffusion of sugar molecules toward the membrane surfaces at elevated temperature because (i) the sugar distributions were initially preequilibrated for 5 ns at 500 K and (ii) the sugar diffusion is not dramatically faster at 475 K than at 325 K (Table 1). An increase in the direct interaction between TRH and lipid headgroups upon increasing the temperature has also been suggested by a recent infrared spectroscopic study of a binary lipid mixture in the absence and presence of TRH.[18]

Another difference observed in the systems containing sugars at 475 K is the higher proportion of sugar−headgroup H-bonds involving the ester oxygens (Table 5). This is compatible with a more significant intercalation of the sugar molecules between lipid chains (more space available due to an increased area per lipid). As was the case at 325 K, the relative contribution of sugar−ester H-bonds is higher for GLC as compared to MLT or TRH.

The nature of the sugar−DPPC H-bonds is analyzed in more detail in Table 6. Sugar molecules are able to form multiple H-bonds simultaneously, sometimes with the same DPPC molecule and sometimes with distinct ones. Configurations where a single TRH, MLT, or GLC molecule forms as many as seven H-bonds with lipid molecules (taking into account donor and acceptor hydroxyl groups) have been observed in the simulations. Comparing the occurrences of the different

TABLE 6: Average Number of TRH, MLT, and GLC Molecules Forming a Specific H-Bonding Pattern[a] with DPPC Molecules during the Simulations at Either 325 or 475 K

pattern	TRH 325 K	TRH 475 K	MLT 325 K	MLT 475 K	GLC 325 K	GLC 475 K
0	73.91	57.53	67.99	51.89	173.10	144.76
1	26.51	24.08	25.42	26.09	33.60	42.15
11	11.40	12.71	13.36	13.63	16.37	13.61
111	3.00	4.11	3.78	4.44	3.83	2.60
1111	0.75	0.74	1.44	1.01	0.20	0.22
2	6.11	8.67	6.32	9.55	14.17	26.28
21	3.03	8.57	4.54	9.43	8.66	17.04
211	1.99	4.75	1.85	5.26	2.67	4.28
22	0.01	0.40	0.41	0.29	0.03	0.32
3	0.51	1.10	0.66	1.23	2.10	2.19
31	0.11	1.20	0.79	1.17	0.96	1.09
4	0.01	0.10	0.02	0.11	0.04	0.05
others	0.64	4.02	1.40	3.87	0.27	1.02
total	128	128	128	128	256	256

[a] A pattern is noted by series of integers (in descending order) indicating the number of H-bonds formed between a sugar molecule and each one of a series of distinct DPPC molecules. A zero indicates molecules forming no H-bonds to DPPC, while "others" indicates sugar molecules forming five or more H-bonds. The averages are calculated over the interval 2.0−6.0 ns for each simulation.

TABLE 7: Average Number of TRH, MLT, and GLC Molecules Bridging a Specific Number of Distinct DPPC Molecules through (Possibly Multiple) H-Bonds during the Simulations at Either 325 or 475 K[a]

degree of bridging	TRH 325 K	TRH 475 K	contribution [%]	MLT 325 K	MLT 475 K	contribution [%]	GLC 325 K	GLC 475 K	contribution [%]
0	73.91	57.53	0.00	67.99	51.89	0.00	173.10	144.76	0.00
1	33.46	33.95	0.79	32.42	36.98	8.67	49.91	71.07	34.26
2	14.55	23.06	27.28	19.45	24.69	19.92	26.03	32.11	19.69
3	5.17	10.10	23.71	6.08	10.90	27.49	6.58	7.59	4.91
4	1.18	2.79	10.32	1.99	3.04	7.98	0.76	0.47	-1.88
others	0.03	0.55	4.17	0.05	0.47	3.99	0.00	0.01	0.08
total	128	128	66.27	128	128	68.05	256	256	57.06

[a] A zero indicates molecules forming no H-bonds to DPPC, while "others" indicates sugar molecules H-bonded to five or more distinct DPPC molecules. The relative contribution of each bridging pattern (assuming a minimum of one H-bond to each of the bridged DPPC molecules) to the increase in the total number of sugar−DPPC H-bonds upon increasing the temperature from 325 to 475 K (i.e., 65%, 45%, and 40% for TRH, MLT, and GLC, respectively) is also indicated. The averages are calculated over the interval 2.0−6.0 ns for each simulation.

H-bonding patterns at 325 and 475 K, interesting observations can be made. At 325 K most of the sugar molecules (87%, 83%, or 87% for TRH, MLT, or GLC, respectively) belong to the patterns "0", "1", or "11", that is, are either not H-bonded to the bilayer or form a single H-bond with one or two distinct DPPC molecules. Upon increasing the temperature, the occurrences of these three patterns are reduced (to 74%, 72%, or 78% for TRH, MLT, or GLC, respectively). In contrast, the occurrences of all other patterns, involving multiple H-bonds to the same DPPC molecule and/or the bridging of more than two DPPC molecules by a common sugar molecule, nearly systematically increase (the only exception being patterns "111" for GLC, "1111" for TRH and MLT, and "22" for MLT). The occurrence of sugar molecules with a specific degree of bridging (i.e., forming at least one H-bond with a given number of distinct DPPC molecules) is analyzed in Table 7. The results clearly evidence that the dominant contribution to the increase in the number of TRH−DPPC and MLT−DPPC H-bonds upon increasing the temperature is an increase in the degree of bridging of the sugar molecules and, in particular, an increased likelihood of finding TRH or MLT molecules H-bonded to three or more distinct DPPC molecules. The changes in the degree of bridging account for 66% or 68% of the increase in the total number of TRH−DPPC or MLT−DPPC H-bonds, respectively. The remaining contribution is due to an increase in the multiplicity of H-bonds between sugar and DPPC molecules. For the systems with GLC, the picture is slightly different. Here, the dominant contribution to the increase in the number of sugar−DPPC H-bonds upon increasing the temperature comes from GLC molecules H-bonded to one or two DPPC molecules only. Although GLC molecules binding three (or sometimes more) distinct DPPC molecules can be found in the system at the two temperatures, their contribution to the increase in the number of H-bonds upon increasing the temperature is much smaller as compared to the case of the two disaccharides (Table 7). This result is certainly correlated with the smaller number of hydroxyl groups available as H-bonding donors in GLC molecules (5) as compared to the TRH and MLT molecules (8). The presence of H-bonds between sugar and lipid molecules has been evidenced directly in many experimental[14,15,19,20,45,47,66,67] and theoretical studies.[21−25] However, the present simulation results suggest that, although the average number of H-bonds (at similar effective concentrations of hydroxyl groups) are comparable (Tables 2−4; with a somewhat larger number for GLC), these H-bonds are distributed in a very different way for the systems containing mono- or disaccharides (with a larger extent of bridging in the latter case). This observation could be correlated with the more limited ability of GLC to stabilize membranes exposed to stress factors when compared to TRH and MLT,[14,15,42,47,62,63−67] although the poorer glass-forming properties of the monosaccharide also clearly represent an important factor.

Conclusions

The aim of the present study was to investigate and compare the interaction of the disaccharides TRH and MLT, and of the monosaccharide GLC, with a DPPC bilayer at two different temperatures using MD simulations.

At 325 K and in the concentration range considered (2 m for TRH and MLT; 4 m for GLC), it is observed that (i) the

membrane structure and dynamics are not significantly altered by the presence of sugars; (ii) sugar molecules present a high affinity for the membrane surfaces (forming H-bonds with DPPC molecules); and (iii) water is not completely expelled from the bilayer surfaces by the clustering of sugar molecules. In this concentration regime, about one-fifth to one-quarter of the DPPC−water H-bonds occurring in the absence of sugar are replaced by H-bonds to a sugar molecule. About 85% of the sugar molecules either do not form a H-bond to DPPC or form a single H-bond to either one or two distinct DPPC molecules.

At 475 K, the membrane initially undergoes a significant lateral expansion. The subsequent behavior depends crucially on the presence or absence of sugar in the system. In the absence of sugar, the membrane collapses into a structure that cannot be recognized as a bilayer. In the presence of sugars, the bilayer integrity is maintained throughout the simulation. The protective action of sugars appears to be correlated with a significant increase (65%, 45%, or 40% for TRH, MLT, or GLC) in the number of sugar−DPPC H-bonds upon raising the temperature (although the total number of H-bonds between all species decreases by approximately 30%). This suggests that, after the initial thermal expansion of the membrane, sugar molecules intercalate between the lipid headgroups and prevent the collapse of the membrane to an unstructured state through the formation of H-bonds. For the disaccharides, this increase can be dominantly attributed to a large increase in the number of sugar molecules bridging three or more lipid molecules via H-bonds. For the monosaccharide, the increase is principally due to an increase in the number of sugar molecules H-bonded to one or two DPPC molecules. This difference in the H-bonding patterns observed for mono- and disaccharides (in addition to poorer glass-formation properties) may be correlated with the more limited protective ability of the former class of compounds. All sugars significantly increase the order of the lipid chains, leading to increased order parameters (this effect is probably also related with an enhanced alignment of the lipid chains in the bilayer normal direction). The key role played by sugar−DPPC H-bonds in the stabilization of the membrane structure under unfavorable external conditions is in qualitative agreement with the results of several experimental studies.[6,12−20]

When trying to relate the present simulation results to the three main hypotheses for the mechanism underlying the bioprotective action of sugars (water replacement, water entrapment, or vitrification), one should keep in mind that these simulations only probe a given type of biostructure (pure DPPC membrane) and environmental stress (artificially elevated temperature), a given concentration range (0−4 m), and a rather short time scale (6 ns). In addition, it is important to recall that the three above-mentioned hypotheses have been formulated essentially on the basis of experimental data involving completely (or almost completely) dehydrated biostructures. Keeping these restrictions in mind, the present simulation results showing the membrane preservation at elevated temperature (by TRH, MLT, and, to a lesser extent, GLC) are best interpreted in the context of the water-replacement hypothesis, because (i) direct H-bonding interactions between DPPC and sugar molecules are observed and (ii) these interactions are enhanced when the membrane is subject to thermal stress. However, in the concentration regime considered, water is only partially replaced by sugar molecules, and only a fraction (about one-fifth to one-quarter at 325 K and up to twice as much at 475 K) of the DPPC−water H-bonds occurring in the absence of sugar are substituted by sugar−DPPC H-bonds. The presence of direct H-bonding interactions between sugars and phospholipid headgroups even in an excess of water has been observed in previous simulations[21−25] and is supported by some experimental evidence[16,17] (see, however, ref 63). Upon increasing the sugar concentration, it seems likely that a complete water replacement might occur when reaching conditions of almost complete dehydration.

Acknowledgment. Financial support by the Swiss National Foundation grant #21-105397 is gratefully acknowledged. We would like to thank Mika Kastenholz and Chris Oostenbrink for valuable help with the analysis programs and Roberto D. Lins for helpful discussions.

Supporting Information Available: Results from the simulations involving TRH at 1 m concentration, performed using the latest version of the force field.[80] This material is available free of charge via the Internet at http://pubs.acs.org.

References and Notes

(1) Feofilova, E. P. *Appl. Biochem. Microbiol.* **2003**, *39*, 1−18.
(2) Clegg, J. S. *Comp. Biochem. Physiol., B* **2001**, *128*, 613−624.
(3) Crowe, J. H.; Oliver, A. E.; Tablin, F. *Integr. Comp. Biol.* **2002**, *42*, 497−503.
(4) Crowe, L. M. *Comp. Biochem. Physiol., A* **2002**, *131*, 505−513.
(5) Tunnacliffe, A.; Lapinski, J. *Philos. Trans. R. Soc. London, Ser. B* **2003**, *358*, 1755−1771.
(6) Crowe, J. H.; Crowe, L. M.; Chapman, D. *Science* **1984**, *223*, 701−703.
(7) Crowe, J. H.; Hoekstra, F. A.; Crowe, L. M. *Annu. Rev. Physiol.* **1992**, *54*, 579−599.
(8) Crowe, J. H.; Crowe, L. M.; Carpenter, J. F.; Prestrelski, S.; Hoekstra, F. A.; de Araújo, P.; Panek, A. D. In *Handbook of Physiology*; Dantzler, W. H., Ed.; Oxford University Press: Oxford, 1997; Vol. 2, pp 1445−1477.
(9) Crowe, J. H.; Clegg, J. S.; Crowe, L. M. In *The Properties of Water in Foods (ISO−POW 6)*; Reid, D. S., Ed.; Chapman and Hall: New York, 1998; pp 440−455.
(10) Carpenter, J. F.; Prestrelski, S. J.; Anchordoguy, T. J.; Arakawa, T. In *Formulation and Delivery of Proteins and Peptides*; Cleland, J. L., Langer, R., Eds.; Am. Chem. Soc: Washington, DC, 1994; pp 134−147.
(11) Hoekstra, F. A.; Wolkers, W. F.; Buitink, J.; Golovina, E. A.; Crowe, J. H.; Crowe, L. M. *Comp. Biochem. Physiol., A* **1997**, *117*, 335−341.
(12) Lee, C. W. B.; Waugh, J. S.; Griffin, R. G. *Biochemistry* **1986**, *25*, 3737−3742.
(13) Nakagaki, M.; Nagase, H.; Ueda, H. *J. Membr. Sci.* **1992**, *73*, 173−180.
(14) Tsvetkova, N. M.; Phillips, B. L.; Crowe, L. M.; Crowe, J. H.; Risbud, S. H. *Biophys. J.* **1998**, *75*, 2947−2955.
(15) Nagase, H.; Ueda, H.; Nakagaki, M. *Chem. Pharm. Bull.* **1999**, *47*, 607−610.
(16) Luzardo, M. D.; Amalfa, F.; Nunez, A. M.; Diaz, S.; de Lopez, A. C. B.; Disalvo, E. A. *Biophys. J.* **2000**, *78*, 2452−2458.
(17) Lambruschini, C.; Relini, N.; Ridi, A.; Cordone, L.; Gliozzi, A. *Langmuir* **2000**, *16*, 5467−5470.
(18) Ricker, J. V.; Tsvetkova, N. M.; Wolkers, W. F.; Leidy, C.; Tablin, F.; Longo, M.; Crowe, J. H. *Biophys. J.* **2003**, *84*, 3045−3051.
(19) Hincha, D. K.; Zuther, E.; Hellwege, E. M.; Heyer, A. G. *Glycobiology* **2002**, *12*, 103−110.
(20) Hincha, D. K.; Hagemann, M. *Biochem. J.* **2004**, *383*, 277−283.
(21) Sum, A. K.; Faller, R.; de Pablo, J. J. *Biophys. J.* **2003**, *85*, 2830−2844.
(22) Pereira, C. S.; Lins, R. D.; Chandrasekhar, I.; Freitas, L. C. G.; Hünenberger, P. H. *Biophys. J.* **2004**, *86*, 2273−2285.
(23) Villarreal, M. A.; Diaz, S. B.; Disalvo, E. A.; Montich, G. G. *Langmuir* **2004**, *20*, 7844−7851.
(24) Lee, B. W.; Faller, R.; Sum, A. K.; Vattulainen, I.; Patra, M.; Karttunen, M. *Fluid Phase Equilib.* **2004**, *225*, 63−68.
(25) Skibinsky, A.; Venable, R. M.; Pastor, R. W. *Biophys. J.* **2005**, *89*, 4111−4121.
(26) Belton, P. S.; Gil, A. M. *Biopolymers* **1994**, *34*, 957−961.
(27) Massari, A. M.; Finkelstein, I. J.; McClain, B. L.; Goj, A.; Wen, X.; Bren, K. L.; Loring, R. F.; Fayer, M. D. *J. Am. Chem. Soc.* **2005**, *127*, 14279−14289.
(28) Cottone, G.; Ciccotti, G.; Cordone, L. *J. Chem. Phys.* **2002**, *117*, 9862−9866.

(29) Lins, R. D.; Pereira, C. S.; Hünenberger, P. H. *Proteins: Struct., Funct., Bioinformatics* **2004**, *55*, 177−186.
(30) Giuffrida, S.; Cottone, G.; Cordone, L. *J. Phys. Chem. B* **2004**, *108*, 15415−15421.
(31) Cordone, L.; Cottone, G.; Giuffrida, S.; Palazzo, G.; Venturoli, G.; Viappiani, C. *Biochim. Biophys. Acta-Proteins Proteomics* **2005**, *1749*, 252−281.
(32) Timasheff, S. N. In *Biophysics of Water*; Franks, F., Mathias, S., Eds.; Wiley: New York, 1982; pp 70−72.
(33) Xie, G. F.; Timasheff, S. N. *Biophys. Chem.* **1997**, *64*, 25−43.
(34) Koster, K. L.; Webb, M. S.; Bryant, G. *Biochim. Biophys. Acta* **1994**, *1193*, 143−150.
(35) Koster, K. L.; Lei, Y. P.; Anderson, M.; Martin, S.; Bryant, G. *Biophys. J.* **2000**, *78*, 1932−1946.
(36) Zhang, J.; Steponkus, P. L. *Cryobiology* **1996**, *33*, 625−626.
(37) Sun, W. Q.; Leopold, A. C. *Ann. Bot. (London)* **1994**, *74*, 601−604.
(38) Sun, W. Q.; Leopold, A. C. *Comp. Biochem. Physiol., A* **1997**, *117*, 327−333.
(39) Sun, W. Q.; Irving, T. C.; Leopold, A. C. *Physiol. Plant.* **1994**, *90*, 621−628.
(40) Sun, W. Q.; Leopold, A. C.; Crowe, L. M.; Crowe, J. H. *Biophys. J.* **1996**, *70*, 1769−1776.
(41) Williams, R. J.; Leopold, A. C. *Plant. Physiol.* **1989**, *89*, 977−981.
(42) Wolfe, J.; Bryant, G. *Cryobiology* **1999**, *39*, 103−129.
(43) Crowe, J. H.; Carpenter, J. F.; Crowe, L. M. *Annu. Rev. Physiol.* **1998**, *60*, 73−103.
(44) Crowe, J. H.; Leslie, S. B.; Crowe, L. M. *Cryobiology* **1994**, *31*, 355−366.
(45) Crowe, J. H.; Hoekstra, F. A.; Nguyen, K. H. N.; Crowe, L. M. *Biochim. Biophys. Acta* **1996**, *1280*, 187−196.
(46) Kodama, M.; Kuwabara, M.; Seki, S. *Biochim. Biophys. Acta* **1982**, *689*, 567−570.
(47) Crowe, J. H.; Oliver, A. E.; Hoekstra, F. A.; Crowe, L. M. *Cryobiology* **1997**, *35*, 20−30.
(48) Miller, D. P.; de Pablo, J. J. *J. Phys. Chem.* **2000**, *104*, 8876−8883.
(49) Crowe, J. H.; Crowe, L. M.; Oliver, A. E.; Tsvetkova, N.; Wolkers, W.; Tablin, F. *Cryobiology* **2001**, *43*, 89−105.
(50) Singer, M. A.; Lindquist, S. *Trends Biotechnol.* **1998**, *16*, 460−468.
(51) Damore, T. G.; Crumplen, R. G.; Stewart, G. G. *J. Ind. Microbiol.* **1991**, *7*, 191−195.
(52) Eleutherio, E. C. A.; Silva, J. T.; Panek, A. *Biochim. Biophys. Acta* **1993**, *1156*, 263−266.
(53) Westh, P.; Ramlov, H. *J. Exp. Zool.* **1991**, *258*, 303−311.
(54) Somme, L. *Eur. J. Entomol.* **1996**, *93*, 349−357.
(55) Madin, K. A. C.; Crowe, J. *J. Exp. Zool.* **1975**, *193*, 335−342.
(56) Behm, C. A. *Intern. J. Parasitol.* **1997**, *27*, 215−229.
(57) Scott, P. *Ann. Bot.* **2000**, *85*, 159−166.
(58) Wingler, A. *Phytochemistry* **2002**, *60*, 437−440.
(59) Clegg, J. S. *Comp. Biochem. Physiol.* **1965**, *14*, 135−143.
(60) Clegg, J. S. *J. Exp. Biol.* **1997**, *200*, 467−475.
(61) Clegg, J. S.; Jackson, S. A. *FEBS Lett.* **1992**, *303*, 45−47.
(62) Crowe, L. M.; Mouradian, R.; Crowe, J. H.; Jackson, S. A.; Womersley, C. *Biochim. Biophys. Acta* **1984**, *769*, 141−150.
(63) Crowe, L. M.; Womersley, C.; Crowe, J. H.; Reid, D.; Appel, L.; Rudolph, A. *Biochim. Biophys. Acta* **1986**, *861*, 131−140.
(64) Imamura, K.; Ogawa, T.; Sakiyama, T.; Nakanishi, K. *J. Pharm. Sci.* **2002**, *92*, 266−274.
(65) Miyajima, K. *Adv. Drug Delivery Rev.* **1997**, *24*, 151−159.
(66) Nagase, H.; Ueda, H.; Nakagaki, M. *Biochim. Biophys. Acta* **1997**, *1328*, 197−206.
(67) Suzuki, T.; Komatsu, H.; Miyajima, K. *Biochim. Biophys. Acta* **1996**, *1278*, 176−182.
(68) Mason, P. E.; Neilson, G. W.; Barnes, A. C.; Enderby, J. E.; Brady, J. W.; Saboungi, M. L. *J. Chem. Phys.* **2003**, *119*, 3347−3353.
(69) Branca, C.; Magazu, S.; Maisano, G.; Migliardo, P. *J. Chem. Phys.* **1999**, *111*, 281−287.
(70) Branca, C.; Magazu, S.; Maisano, G.; Migliardo, P. *J. Biol. Phys.* **2000**, *26*, 295−306.
(71) Magazu, S.; Migliardo, F.; Mondelli, C.; Vadala, M. *Carbohydr. Res.* **2005**, *340*, 2796−2801.
(72) Lerbret, A.; Bordat, P.; Affouard, F.; Guinet, Y.; Hedoux, A.; Paccou, L.; Prevost, D.; Descamps, M. *Carbohydr. Res.* **2005**, *340*, 881−887.
(73) Lee, S. L.; Debenedetti, P. G.; Errington, J. R. *J. Chem. Phys.* **2005**, *122*, Art. No. 204511.
(74) Lerbret, A.; Bordat, P.; Affouard, F.; Descamps, M.; Migliardo, F. *J. Phys. Chem. B* **2005**, *109*, 11046−11057.
(75) Sakurai, M.; Murata, M.; Inoue, Y.; Hino, A.; Kobayashi, S. *Bull. Chem. Soc. Jpn.* **1997**, *70*, 847−858.
(76) Conrad, P. B.; de Pablo, J. J. *J. Phys. Chem. A* **1999**, *103*, 4049−4055.
(77) Engelsen, S. B.; Monteiro, C.; de Penhoat, C. H.; Perez, S. *Biophys. Chem.* **2001**, *93*, 103−127.
(78) van Gunsteren, W. F.; Billeter, S. R.; Eising, A. A.; Hünenberger, P. H.; Krüger, P.; Mark, A. E.; Scott, W. R. P.; Tironi, I. G. Biomolecular Simulation: the GROMOS96 manual and user guide. Hochschulverlag an der ETH Zürich/Biomos, Zürich/Groningen, 1996.
(79) Chandrasekhar, I.; Kastenholz, M.; Lins, R. D.; Oostenbrink, C.; Schuler, L. D.; Tieleman, D. P.; van Gunsteren, W. F. *Eur. Biophys. J.* **2003**, *32*, 67−77.
(80) Lins, R. D.; Hünenberger, P. H. *J. Comput. Chem.* **2005**, *26*, 1400−1412.
(81) Berendsen, H. J. C.; Postma, J. P. M.; van Gunsteren, W. F.; Hermans, J. In *Intermolecular Forces*; Pullman, B., Ed.; Reidel: Dordrecht, 1981; pp 331−342.
(82) Angyal, S. J.; Bethell, G. S. *Aust. J. Chem.* **1972**, *25*, 1695−1710.
(83) Nagle, J. F.; Tristam-Nagle, S. *Biochim. Biophys. Acta* **2000**, *1469*, 159−195.
(84) Takahashi, H.; Ohmae, H.; Hatta, I. *Biophys. J.* **1997**, *73*, 3030−3038.
(85) Douliez, J. P.; Leonard, A.; Dufourc, E. J. *Biophys. J.* **1995**, *68*, 1727−1739.
(86) Ekdawi-Sever, N.; de Pablo, J. J.; Feick, E.; von Meerwall, E. *J. Phys. Chem. A* **2003**, *107*, 936−943.
(87) Sackmann, E. In *Handbook of Biological Physics, Structure and Dynamics of Membranes*; Lipowsky, R., Sackman, E., Eds.; Elsevier: Amsterdam, 1995; Vol. 1A, pp 213−304.
(88) Alonso-Romanowski, S.; Biondi, A. C.; Disalvo, E. A. *J. Membr. Biol.* **1989**, *108*, 1−11.
(89) Doxastakis, M.; Sum, A. K.; de Pablo, J. J. *J. Phys. Chem. B* **2005**, *109*, 24173−24181.